LBNL-42677

ERNEST ORLANDO LAWRENCE
BERKELEY NATIONAL LABORATORY

Three-Dimensional Electromagnetic Modeling in the Laplace Domain

Hideki Mizunaga, Ki Ha Lee, and Hee Joon Kim

Earth Sciences Division

January 1999

REFERENCE COPY
Does Not
Circulate
Bldg. 50 Library - Ref.
Lawrence Berkeley National Laboratory

Copy 1

LBNL-42677

DISCLAIMER

This document was prepared as an account of work sponsored by the United States Government. While this document is believed to contain correct information, neither the United States Government nor any agency thereof, nor the Regents of the University of California, nor any of their employees, makes any warranty, express or implied, or assumes any legal responsibility for the accuracy, completeness, or usefulness of any information, apparatus, product, or process disclosed, or represents that its use would not infringe privately owned rights. Reference herein to any specific commercial product, process, or service by its trade name, trademark, manufacturer, or otherwise, does not necessarily constitute or imply its endorsement, recommendation, or favoring by the United States Government or any agency thereof, or the Regents of the University of California. The views and opinions of authors expressed herein do not necessarily state or reflect those of the United States Government or any agency thereof or the Regents of the University of California.

LBNL-42677

Three-Dimensional Electromagnetic Modeling in the Laplace Domain

Hideki Mizunaga,[1]* Ki Ha Lee,[1] and Hee Joon Kim[2]

[1]Earth Sciences Division
Ernest Orlando Lawrence Berkeley National Laboratory
University of California
Berkeley, California 94720

[2]Pukyong National University
Pusan 608-737, Korea

January 1999

*On leave from Kyushu University, Fukuoka 812-8581, Japan

This work was supported in part by the Office of Science, Office of Basic Energy Sciences, Engineering and Geosciences Division, of the U.S. Department of Energy under Contract No. DE-AC03-76SF00098.

Three-dimensional electromagnetic modeling in the Laplace domain

Introduction

In modeling electromagnetic responses, Maxwell's equations in the frequency domain are popular and have been widely used (Nabighian, 1994; Newman and Alumbaugh, 1995; Smith, 1996, to list a few). Recently, electromagnetic modeling in the time domain using the finite difference (FDTD) method (Wang and Hohmann, 1993) has also been used to study transient electromagnetic interactions in the conductive medium.

This paper presents a new technique to compute the electromagnetic response of three-dimensional (3-D) structures. The proposed new method is based on transforming Maxwell's equations to the Laplace domain. For each discrete Laplace variable, Maxwell's equations are discretized in 3-D using the staggered grid and the finite difference method (FDM). The resulting system of equations is then solved for the fields using the incomplete Cholesky conjugate gradient (ICCG) method.

The new method is particularly effective in saving computer memory since all the operations are carried out in real numbers. For the same reason, the computing speed is faster than frequency domain modeling. The proposed approach can be an extremely useful tool in developing an inversion algorithm using the time domain data.

Maxwell's equations in the Laplace domain

The coupled space and time dependent electromagnetic fields are described by Maxwell's equations as

$$\nabla \times \mathbf{E}(\mathbf{r},t) = -\mu \frac{\partial \mathbf{H}(\mathbf{r},t)}{\partial t} - \mu \frac{\partial \mathbf{M}(\mathbf{r},t)}{\partial t} \tag{1}$$

$$\nabla \times \mathbf{H}(\mathbf{r},t) = \varepsilon \frac{\partial \mathbf{E}(\mathbf{r},t)}{\partial t} + \sigma(\mathbf{r})\mathbf{E}(\mathbf{r},t) + \mathbf{J}(\mathbf{r},t) \tag{2}$$

where **E** and **H** are the electric and magnetic fields respectively, **M** and **J** are the impressed magnetic and electric currents density, respectively, μ is the magnetic permeability, σ is the electric conductivity and ε is the electric permittivity.

If we perform a Fourier transformation on equations (1) and (2), we obtain Maxwell's equations in the frequency domain

$$\nabla \times \boldsymbol{E}(\mathbf{r},\omega) = -i\omega\mu \boldsymbol{H}(\mathbf{r},\omega) - i\omega\mu \boldsymbol{M}(\mathbf{r},\omega) \tag{3}$$

$$\nabla \times \boldsymbol{H}(\mathbf{r},\omega) = \{\sigma(\mathbf{r}) + i\omega\varepsilon\}\boldsymbol{E}(\mathbf{r},\omega) + \boldsymbol{J}(\mathbf{r},\omega) \tag{4}$$

Equations (3) and (4) are well-known formulas and widely used for electromagnetic modeling.

In this paper Laplace transformation is used instead of Fourier transformation. The Laplace transform of the time domain function F(t) is defined as

$$f(s) = \int_0^\infty F(t)e^{-st}dt \tag{5}$$

If we perform Laplace transformation to equations (1) and (2) with the following initial condition,

$$\mathbf{E}(\mathbf{r},0) = \mathbf{H}(\mathbf{r},0) = \mathbf{M}(\mathbf{r},0) = \mathbf{J}(\mathbf{r},0) = 0 \tag{6}$$

we obtain Maxwell's equations in the Laplace domain (Chen, 1985)

$$\nabla \times \mathbf{e}(\mathbf{r},s) = -\mu s\mathbf{h}(\mathbf{r},s) - \mu s\mathbf{m}(\mathbf{r},s) \tag{7}$$

$$\nabla \times \mathbf{h}(\mathbf{r},s) = \{\sigma(\mathbf{r}) + \varepsilon s\}\mathbf{e}(\mathbf{r},s) + \mathbf{j}(\mathbf{r},s) \tag{8}$$

where **e**, **h**, **m** and **j** denote the Laplace transforms of **E**, **H**, **M** and **J**, respectively.

Electromagnetic fields in a homogeneous half space

Let us consider a homogeneous half space model with a vertical magnetic dipole (VMD) source illustrated in Fig.1. We write Maxwell's equations in the air (z<0)

$$\nabla \times \mathbf{e}_A(\mathbf{r},s) = -\mu_0 s\mathbf{h}_A(\mathbf{r},s) - \mu_0 s\mathbf{m}(\mathbf{r},s) \tag{9}$$

$$\nabla \times \mathbf{h}_A(\mathbf{r},s) = \{\sigma_0(\mathbf{r}) + \varepsilon_0 s\}\mathbf{e}_A(\mathbf{r},s) \tag{10}$$

where $\mathbf{e}_A$ and $\mathbf{h}_A$ are the electric and magnetic fields in the air, respectively, μ_0, σ_0 and ε_0 are the magnetic permeability, the electric conductivity and the electric permittivity in the air, respectively. We can also write Maxwell's equations in the earth (z>0)

$$\nabla \times \mathbf{e}_E(\mathbf{r},s) = -\mu_1 s\mathbf{h}_E(\mathbf{r},s) \tag{11}$$

$$\nabla \times \mathbf{h}_E(\mathbf{r},s) = \{\sigma_1(\mathbf{r}) + \varepsilon_1 s\}\mathbf{e}_E(\mathbf{r},s) \tag{12}$$

where $\mathbf{e}_E$ and $\mathbf{h}_E$ are the electric and magnetic fields in the earth respectively, μ_1, σ_1 and ε_1 are the magnetic permeability, the electric conductivity and the electric permittivity in the earth respectively.

In the case of a VMD source illustrated in Fig.2, we obtain the following Helmholtz equations from equations (9) through (12).

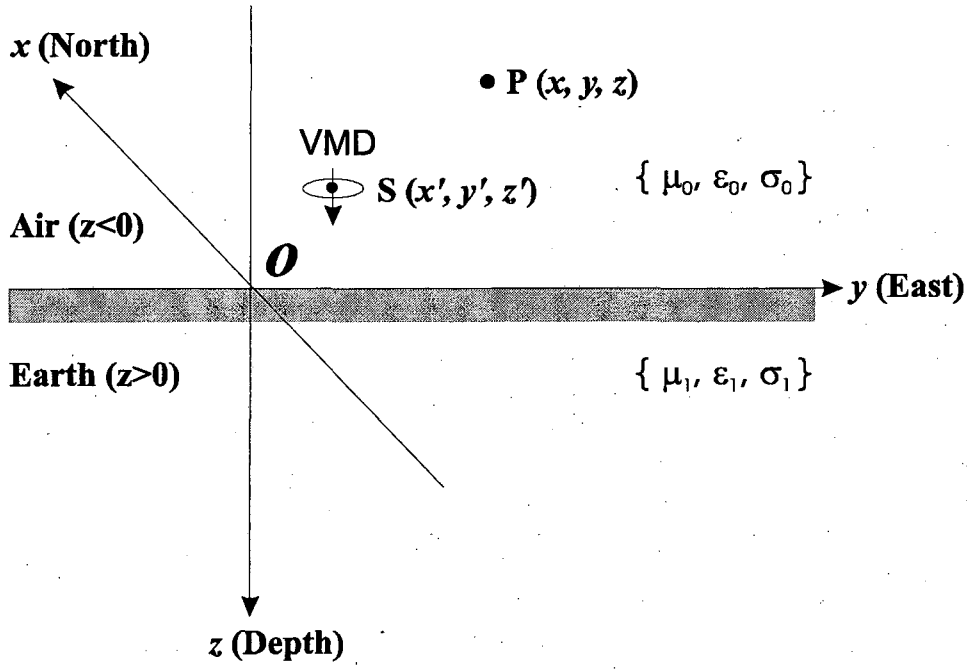

Fig.1 Homogeneous half space model with vertical magnetic dipole source.

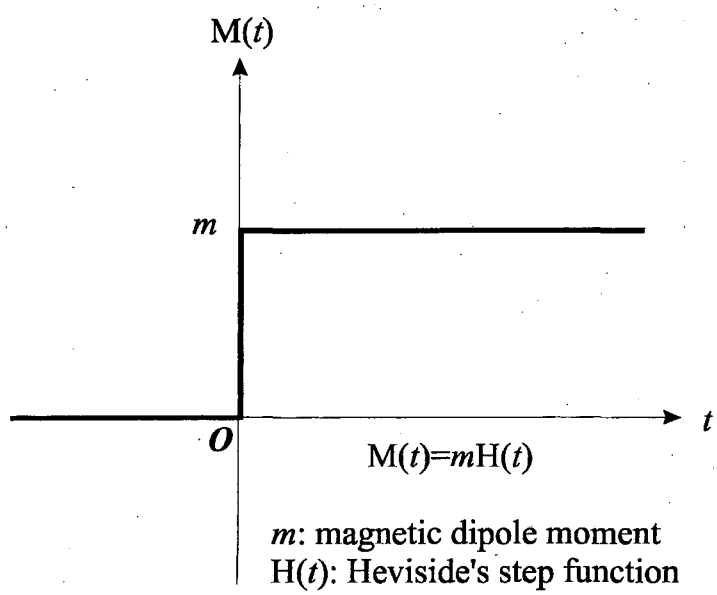

Fig.2 Magnetic dipole function used as a VMD source.

$$\nabla^2 F_A + k_0{}^2 F_A = -\mu_0 m \delta(x-x')\delta(y-y')\delta(z-z') \tag{13}$$

$$\nabla^2 F_E + k_1{}^2 F_E = 0 \tag{14}$$

where k_0 and k_1 are given by

$$k_0{}^2 = -\mu_0\sigma_0 s - \mu_0\varepsilon_0 s^2 \tag{15}$$

$$k_1{}^2 = -\mu_1\sigma_1 s - \mu_1\varepsilon_1 s^2 \tag{16}$$

Here F_A and F_E denote the scalar potentials in the air and the earth, respectively.

Using boundary conditions at the air-earth interface, the theoretical formulas for scalar potentials are obtained as follows:

$$F_A = \frac{\mu_0 m}{4\pi}\int_0^\infty \left[e^{-\gamma_0|z-z'|} + \frac{\gamma_0-\gamma_1}{\gamma_0+\gamma_1} e^{\gamma_0(z+z')} \right] \frac{\lambda}{\gamma_0} J_0(\lambda r) d\lambda \tag{17}$$

$$F_E = \frac{\mu_0 m}{2\pi}\int_0^\infty \frac{1}{\gamma_0+\gamma_1} e^{-\gamma_1 z+\gamma_0 z'} \lambda J_0(\lambda r) d\lambda \tag{18}$$

where γ_0 and γ_1 are defined as

$$\gamma_0 = \sqrt{\lambda^2 + \mu_0\sigma_0 s + \mu_0\varepsilon_0 s^2}, \quad \gamma_1 = \sqrt{\lambda^2 + \mu_1\sigma_1 s + \mu_1\varepsilon_1 s^2} \tag{19}$$

and the horizontal distance r is given by

$$r = \sqrt{(x-x')^2 + (y-y')^2}\,. \tag{20}$$

Each component of the electric and magnetic fields can be derived using the following relations.

$$e_{A,x} = -\frac{\partial F_A}{\partial y}, \qquad e_{A,y} = \frac{\partial F_A}{\partial x}, \qquad e_{A,z} = 0 \tag{21}$$

$$h_{A,x} = \frac{1}{\mu_0 s}\frac{\partial^2 F_A}{\partial x \partial z}, \; h_{A,y} = \frac{1}{\mu_0 s}\frac{\partial^2 F_A}{\partial y \partial z}, \; h_{A,z} = \frac{1}{\mu_0 s}\left(\frac{\partial^2}{\partial z^2} + k_0{}^2\right) F_A \tag{22}$$

$$e_{E,x} = -\frac{\partial F_E}{\partial y}, \qquad e_{E,y} = \frac{\partial F_E}{\partial x}, \qquad e_{E,z} = 0 \tag{23}$$

$$h_{E,x} = \frac{1}{\mu_1 s}\frac{\partial^2 F_E}{\partial x \partial z},\ h_{E,y} = \frac{1}{\mu_1 s}\frac{\partial^2 F_E}{\partial y \partial z},\ h_{E,z} = \frac{1}{\mu_1 s}\left(\frac{\partial^2}{\partial z^2} + k_1^{\ 2}\right)F_E \tag{24}$$

where $e_{A,x}$, $e_{A,y}$ and $e_{A,z}$ denote the *x*, *y* and *z* components of electric fields in the air, $h_{A,x}$, $h_{A,y}$ and $h_{A,z}$ denote the *x*, *y* and *z* components of magnetic fields in the air, $e_{E,x}$, $e_{E,y}$ and $e_{E,z}$ denote the *x*, *y* and *z* components of electric fields in the earth, $h_{E,x}$, $h_{E,y}$ and $h_{E,z}$ denote the *x*, *y* and *z* components of magnetic fields in the earth respectively.

Assuming $\mu_1 = \mu_0$ and $\varepsilon_1 = \varepsilon_0$, we obtain the theoretical formulas for the electromagnetic fields both in the air and earth using the relations in equations (21) through (24) as follows.

In the air (z<0), we obtain

$$e_{A,x} = \frac{\mu_0 m(y-y')}{4\pi r}\int_0^\infty \left[e^{-\gamma_0|z-z'|} + \frac{\gamma_0-\gamma_1}{\gamma_0+\gamma_1}e^{\gamma_0(z+z')}\right]\frac{\lambda^2}{\gamma_0}J_1(\lambda r)d\lambda \tag{25}$$

$$e_{A,y} = -\frac{\mu_0 m(x-x')}{4\pi r}\int_0^\infty \left[e^{-\gamma_0|z-z'|} + \frac{\gamma_0-\gamma_1}{\gamma_0+\gamma_1}e^{\gamma_0(z+z')}\right]\frac{\lambda^2}{\gamma_0}J_1(\lambda r)d\lambda \tag{26}$$

$$e_{A,z} = 0 \tag{27}$$

$$h_{A,x} = \frac{m(x-x')}{4\pi r s}\int_0^\infty \left[\frac{z-z'}{|z-z'|}e^{-\gamma_0|z-z'|} - \frac{\gamma_0-\gamma_1}{\gamma_0+\gamma_1}e^{\gamma_0(z+z')}\right]\lambda^2 J_1(\lambda r)d\lambda \tag{28}$$

$$h_{A,y} = \frac{m(y-y')}{4\pi r s}\int_0^\infty \left[\frac{z-z'}{|z-z'|}e^{-\gamma_0|z-z'|} - \frac{\gamma_0-\gamma_1}{\gamma_0+\gamma_1}e^{\gamma_0(z+z')}\right]\lambda^2 J_1(\lambda r)d\lambda \tag{29}$$

$$h_{A,z} = \frac{m}{4\pi s}\int_0^\infty \left[e^{-\gamma_0|z-z'|} + \frac{\gamma_0-\gamma_1}{\gamma_0+\gamma_1}e^{\gamma_0(z+z')}\right]\frac{\lambda^3}{\gamma_0}J_0(\lambda r)d\lambda \tag{30}$$

In the earth (z>0), following equations are obtained

$$e_{E,x} = \frac{\mu_0 m(y-y')}{2\pi r}\int_0^\infty \frac{1}{\gamma_0+\gamma_1}e^{-\gamma_1 z+\gamma_0 z'}\lambda^2 J_1(\lambda r)d\lambda \tag{31}$$

$$e_{E,y} = -\frac{\mu_0 m(x-x')}{2\pi r}\int_0^\infty \frac{1}{\gamma_0+\gamma_1}e^{-\gamma_1 z+\gamma_0 z'}\lambda^2 J_1(\lambda r)d\lambda \tag{32}$$

$$e_{E,z} = 0 \tag{33}$$

$$h_{E,x} = \frac{m(x-x')}{2\pi rs} \int_0^\infty \frac{\gamma_1}{\gamma_0 + \gamma_1} e^{-\gamma_1 z + \gamma_0 z'} \lambda^2 J_1(\lambda r) d\lambda \tag{34}$$

$$h_{E,y} = \frac{m(y-y')}{2\pi rs} \int_0^\infty \frac{\gamma_1}{\gamma_0 + \gamma_1} e^{-\gamma_1 z + \gamma_0 z'} \lambda^2 J_1(\lambda r) d\lambda \tag{35}$$

$$h_{E,z} = \frac{m}{2\pi s} \int_0^\infty \frac{1}{\gamma_0 + \gamma_1} e^{-\gamma_1 z + \gamma_0 z'} \lambda^3 J_0(\lambda r) d\lambda \tag{36}$$

Finite difference method using Staggered grid

We applied the finite difference method using a staggered grid to discretize the three-dimensional subsurface structure. In the discretization, Maxwell's equations for the secondary electromagnetic field are used because the source for the secondary field is smoother than that for the primary field, and fine spatial discretization is not required around the primary source.

Maxwell's equations with an impressed magnetic source in the Laplace domain become

$$\nabla \times \mathbf{e} = -\mu s \mathbf{h} - \mu s \mathbf{m} \tag{37}$$

$$\nabla \times \mathbf{h} = (\sigma + \varepsilon s) \mathbf{e} \tag{38}$$

The total electromagnetic fields are expressed as the sum of the primary field and the secondary field.

$$\mathbf{e} = \mathbf{e}^{(P)} + \mathbf{e}^{(S)} \tag{39}$$

$$\mathbf{h} = \mathbf{h}^{(P)} + \mathbf{h}^{(S)} \tag{40}$$

where suffix $^{(P)}$ and $^{(S)}$ represent the primary and secondary fields, respectively. The primary electromagnetic fields satisfy the following equations.

$$\nabla \times \mathbf{e}^{(P)} = -\mu s \mathbf{h}^{(P)} - \mu s \mathbf{m} \tag{41}$$

$$\nabla \times \mathbf{h}^{(P)} = (\sigma_* + \varepsilon s) \mathbf{e}^{(P)} \tag{42}$$

where σ_* is the "normal" (layered-earth) conductivity with the body not present. Substituting equations (41) and (42) into equations (37) and (39), we obtain Maxwell's equations for the secondary fields as

$$\nabla \times \mathbf{e}^{(S)} = -\mu s \mathbf{h}^{(S)} \tag{43}$$

$$\nabla \times \mathbf{h}^{(S)} = \sigma \mathbf{e}^{(S)} + (\sigma - \sigma_*) \mathbf{e}^{(P)} \tag{44}$$

Taking the curl of equation (44) and substituting the result into equation (43), we obtain the second-order partial differential equation for the electric field

$$\nabla \times \nabla \times \mathbf{e}^{(S)} + \mu s(\sigma + \varepsilon s)\mathbf{e}^{(S)} = -\mu s(\sigma - \sigma_*)\mathbf{e}^{(P)} \tag{45}$$

Using the relationship $\nabla \times \nabla \times \mathbf{A} = -\nabla^2 \mathbf{A} + \nabla(\nabla \cdot \mathbf{A})$, equation (45) can be rewritten as

$$-\nabla^2 \mathbf{e}^{(S)} + \nabla(\nabla \cdot \mathbf{e}^{(S)}) + \mu s(\sigma + \varepsilon s)\mathbf{e}^{(S)} = -\mu s(\sigma - \sigma_*)\mathbf{e}^{(P)}. \tag{46}$$

Each component of equation (46) can be given by

$$\begin{aligned} &-\frac{\partial^2 e_x^{(S)}}{\partial y^2} - \frac{\partial^2 e_x^{(S)}}{\partial z^2} + \frac{\partial^2 e_y^{(S)}}{\partial x \partial y} + \frac{\partial^2 e_z^{(S)}}{\partial x \partial z} + \mu s(\sigma_x + \varepsilon s)e_x^{(S)} \\ &\quad = -\mu s(\sigma_x - \sigma_*)e_x^{(P)} \end{aligned} \tag{47}$$

$$\begin{aligned} &-\frac{\partial^2 e_y^{(S)}}{\partial x^2} - \frac{\partial^2 e_y^{(S)}}{\partial z^2} + \frac{\partial^2 e_x^{(S)}}{\partial y \partial x} + \frac{\partial^2 e_z^{(S)}}{\partial y \partial z} + \mu s(\sigma_y + \varepsilon s)e_y^{(S)} \\ &\quad = -\mu s(\sigma_y - \sigma_*)e_y^{(P)} \end{aligned} \tag{48}$$

$$\begin{aligned} &-\frac{\partial^2 e_z^{(S)}}{\partial x^2} - \frac{\partial^2 e_z^{(S)}}{\partial y^2} + \frac{\partial^2 e_x^{(S)}}{\partial z \partial x} + \frac{\partial^2 e_y^{(S)}}{\partial z \partial y} + \mu s(\sigma_z + \varepsilon s)e_z^{(S)} \\ &\quad = 0 \end{aligned} \tag{49}$$

In this paper the integral form of equation (47), (48) and (49) are used to discretize 3-D structure.

$$\begin{aligned} &\iiint \left[-\frac{\partial^2 e_x^{(S)}}{\partial y^2} - \frac{\partial^2 e_x^{(S)}}{\partial z^2} + \frac{\partial^2 e_y^{(S)}}{\partial x \partial y} + \frac{\partial^2 e_z^{(S)}}{\partial x \partial z} + \mu s(\sigma_x + \varepsilon s)e_x^{(S)} \right] dxdydz \\ &\quad = \iiint \left[-\mu s(\sigma_x - \sigma_*)e_x^{(P)} \right] dxdydz \end{aligned} \tag{50}$$

$$\begin{aligned} &\iiint \left[-\frac{\partial^2 e_y^{(S)}}{\partial x^2} - \frac{\partial^2 e_y^{(S)}}{\partial z^2} + \frac{\partial^2 e_x^{(S)}}{\partial y \partial x} + \frac{\partial^2 e_z^{(S)}}{\partial y \partial z} + \mu s(\sigma_y + \varepsilon s)e_y^{(S)} \right] dxdydz \\ &\quad = \iiint \left[-\mu s(\sigma_y - \sigma_*)e_y^{(P)} \right] dxdydz \end{aligned} \tag{51}$$

$$\iiint\left[-\frac{\partial^2 e_z^{(S)}}{\partial x^2}-\frac{\partial^2 e_z^{(S)}}{\partial y^2}+\frac{\partial^2 e_x^{(S)}}{\partial z\partial x}+\frac{\partial^2 e_y^{(S)}}{\partial z\partial y}+\mu s(\sigma_z+\varepsilon s)e_z^{(S)}\right]dxdydz \tag{52}$$
$$=0$$

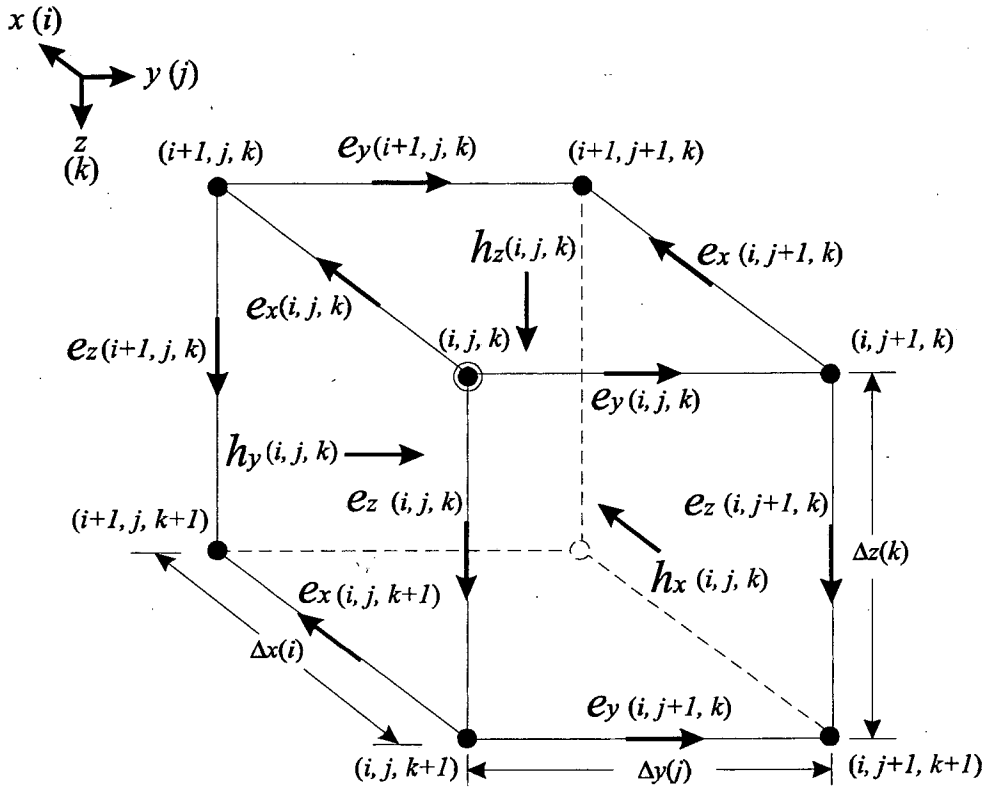

Fig.3 Staggered grid for electromagnetic modeling.

Using the staggered grid illustrated in Fig.3, we can obtain the approximated equations

$$\left[\frac{\Delta x(i)\Delta\bar{z}(k)}{\Delta y(j-1)}+\frac{\Delta x(i)\Delta\bar{z}(k)}{\Delta y(j)}+\mu s\{\bar{\sigma}_x(i,j,k)+\varepsilon s\}\Delta x(i)\Delta\bar{y}(j)\Delta\bar{z}(k)\right.$$
$$\left.+\frac{\Delta x(i)\Delta\bar{y}(j)}{\Delta z(k-1)}+\frac{\Delta x(i)\Delta\bar{y}(j)}{\Delta z(k)}\right]e_x^{(S)}(i,j,k)$$
$$-\frac{\Delta x(i)\Delta\bar{z}(k)}{\Delta y(j-1)}e_x^{(S)}(i,j-1,k)-\frac{\Delta x(i)\Delta\bar{z}(k)}{\Delta y(j)}e_x^{(S)}(i,j+1,k)$$
$$-\frac{\Delta x(i)\Delta\bar{y}(j)}{\Delta z(k-1)}e_x^{(S)}(i,j,k-1)-\frac{\Delta x(i)\Delta\bar{y}(j)}{\Delta z(k)}e_x^{(S)}(i,j,k+1)$$
$$+\Delta\bar{z}(k)\left\{e_y^{(S)}(i+1,j,k)-e_y^{(S)}(i+1,j-1,k)-e_y^{(S)}(i,j,k)+e_y^{(S)}(i,j-1,k)\right\}$$

$$+\Delta\bar{y}(j)\left\{e_z^{(S)}(i+1,j,k)-e_z^{(S)}(i+1,j,k-1)-e_z^{(S)}(i,j,k)+e_z^{(S)}(i,j,k-1)\right\}$$
$$=-\mu s\left\{\bar{\sigma}_x(i,j,k)-\sigma_*\right\}\Delta x(i)\Delta\bar{y}(j)\Delta\bar{z}(k)\,e_x^{(P)}(i,j,k) \tag{53}$$

$$\left[\frac{\Delta y(j)\Delta\bar{z}(k)}{\Delta x(i-1)}+\frac{\Delta y(j)\Delta\bar{z}(k)}{\Delta x(i)}+\mu s\left\{\bar{\sigma}_y(i,j,k)+\varepsilon s\right\}\Delta\bar{x}(i)\Delta y(j)\Delta\bar{z}(k)\right.$$
$$\left.+\frac{\Delta\bar{x}(i)\Delta y(j)}{\Delta z(k-1)}+\frac{\Delta\bar{x}(i)\Delta y(j)}{\Delta z(k)}\right]e_y^{(S)}(i,j,k)$$
$$-\frac{\Delta y(j)\Delta\bar{z}(k)}{\Delta x(i-1)}e_y^{(S)}(i-1,j,k)-\frac{\Delta y(j)\Delta\bar{z}(k)}{\Delta x(i)}e_y^{(S)}(i+1,j,k)$$
$$-\frac{\Delta\bar{x}(i)\Delta y(j)}{\Delta z(k-1)}e_y^{(S)}(i,j,k-1)-\frac{\Delta\bar{x}(i)\Delta y(j)}{\Delta z(k)}e_x^{(S)}(i,j,k+1)$$
$$+\Delta\bar{z}(k)\left\{e_x^{(S)}(i,j+1,k)-e_x^{(S)}(i-1,j+1,k)-e_x^{(S)}(i,j,k)+e_x^{(S)}(i-1,j,k)\right\}$$
$$+\Delta\bar{x}(i)\left\{e_z^{(S)}(i,j+1,k)-e_z^{(S)}(i,j+1,k-1)-e_z^{(S)}(i,j,k)+e_z^{(S)}(i,j,k-1)\right\}$$
$$=-\mu s\left\{\bar{\sigma}_y(i,j,k)-\sigma_*\right\}\Delta\bar{x}(i)\Delta y(j)\Delta\bar{z}(k)\,e_y^{(P)}(i,j,k) \tag{54}$$

$$\left[\frac{\Delta\bar{y}(j)\Delta z(k)}{\Delta x(i-1)}+\frac{\Delta\bar{y}(j)\Delta z(k)}{\Delta x(i)}+\mu s\left\{\bar{\sigma}_z(i,j,k)+\varepsilon s\right\}\Delta\bar{x}(i)\Delta\bar{y}(j)\Delta z(k)\right.$$
$$\left.+\frac{\Delta\bar{x}(i)\Delta z(k)}{\Delta y(j-1)}+\frac{\Delta\bar{x}(i)\Delta z(k)}{\Delta y(j)}\right]e_z^{(S)}(i,j,k)$$
$$-\frac{\Delta\bar{y}(j)\Delta z(k)}{\Delta x(i-1)}e_z^{(S)}(i-1,j,k)-\frac{\Delta\bar{y}(j)\Delta z(k)}{\Delta x(i)}e_x^{(S)}(i+1,j,k)$$
$$-\frac{\Delta\bar{x}(i)\Delta z(k)}{\Delta y(j-1)}e_z^{(S)}(i,j-1,k)-\frac{\Delta\bar{x}(i)\Delta z(k)}{\Delta y(j)}e_z^{(S)}(i,j+1,k)$$
$$+\Delta\bar{y}(j)\left\{e_x^{(S)}(i,j,k+1)-e_x^{(S)}(i-1,j,k+1)-e_x^{(S)}(i,j,k)+e_y^{(S)}(i-1,j,k)\right\}$$
$$+\Delta\bar{x}(i)\left\{e_y^{(S)}(i,j,k+1)-e_y^{(S)}(i,j-1,k+1)-e_y^{(S)}(i,j,k)+e_y^{(S)}(i,j-1,k)\right\}$$
$$=0 \tag{55}$$

where

$$\Delta\bar{x}(i)=\frac{\Delta x(i-1)+\Delta x(i)}{2},\ \Delta\bar{y}(j)=\frac{\Delta y(j-1)+\Delta y(j)}{2},\ \Delta\bar{z}(k)=\frac{\Delta z(k-1)+\Delta z(k)}{2} \tag{56}$$

$$\overline{\sigma}_x(i,j,k) = \frac{\sigma(i,j-1,k-1)\Delta y(j-1)\Delta z(k-1) + \sigma(i,j,k-1)\Delta y(j)\Delta z(k-1)}{\{\Delta y(j-1)+\Delta y(j)\}\{\Delta z(k-1)+\Delta z(k)\}} + \frac{\sigma(i,j-1,k)\Delta y(j-1)\Delta z(k) + \sigma(i,j,k)\Delta y(j)\Delta z(k)}{\{\Delta y(j-1)+\Delta y(j)\}\{\Delta z(k-1)+\Delta z(k)\}} \tag{57}$$

$$\overline{\sigma}_y(i,j,k) = \frac{\sigma(i-1,j,k-1)\Delta x(i-1)\Delta z(k-1) + \sigma(i,j,k-1)\Delta x(i)\Delta z(k-1)}{\{\Delta x(i-1)+\Delta x(i)\}\{\Delta z(k-1)+\Delta z(k)\}} + \frac{\sigma(i-1,j,k)\Delta x(i-1)\Delta z(k) + \sigma(i,j,k)\Delta x(i)\Delta z(k)}{\{\Delta x(i-1)+\Delta x(i)\}\{\Delta z(k-1)+\Delta z(k)\}} \tag{58}$$

$$\overline{\sigma}_z(i,j,k) = \frac{\sigma(i-1,j-1,k)\Delta x(i-1)\Delta y(j-1) + \sigma(i,j-1,k)\Delta x(i)\Delta y(j-1)}{\{\Delta x(i-1)+\Delta x(i)\}\{\Delta y(j-1)+\Delta y(j)\}} + \frac{\sigma(i-1,j,k)\Delta x(i-1)\Delta y(j) + \sigma(i,j,k)\Delta x(i)\Delta y(j)}{\{\Delta x(i-1)+\Delta x(i)\}\{\Delta y(j-1)+\Delta y(j)\}} \tag{59}$$

In previous equations (57) through (59), $\overline{\sigma}_x, \overline{\sigma}_y$ and $\overline{\sigma}_z$ mean the average conductivity in x, y and z directions respectively.

Calculation procedure and boundary conditions

Combining Equations (53) through (55) and boundary conditions result in a linear set of equations that can be written in matrix form

$$\mathbf{A}\,\mathbf{x} = \mathbf{b} \tag{60}$$

where **A** is the coefficient matrix, **x** is the electric field vector which consists of e_x, e_y and e_z, and **b** is the source vector obtained from the primary electric fields. We use the Dirichlet boundary condition in which the secondary field is assumed negligible at the boundary, so

$$e_x^{(s)} = e_y^{(S)} = e_z^{(S)} = 0 \tag{61}$$

on the six boundary surfaces $(x = \pm\infty, y = \pm\infty, z = \pm\infty)$.

New digital linear filters (Guptasarma and Singh, 1997) are used to calculate source terms given by equations (31) and (32). Figures 4 and 5 show the numerical examples of the primary electric and magnetic fields due to the VMD source on the surface of the homogeneous half space. The φ component of electric fields in the air is given by (equations (25) and (26))

$$e_{A,\varphi} = -\frac{y-y'}{r}e_{A,x} + \frac{x-x'}{r}e_{A,y} \tag{62}$$

The z component of magnetic fields is calculated using equation (30).

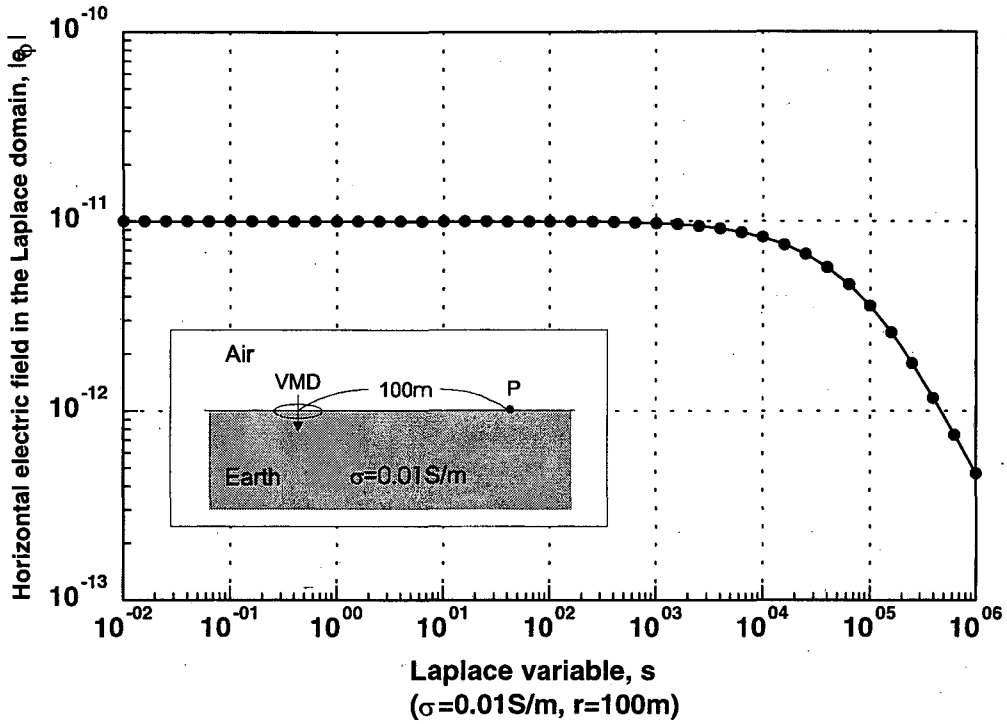

Fig.4 Horizontal electric fields in the Laplace domain due to the VMD source (1A-m^2) on the homogeneous (0.01S/m) half space.

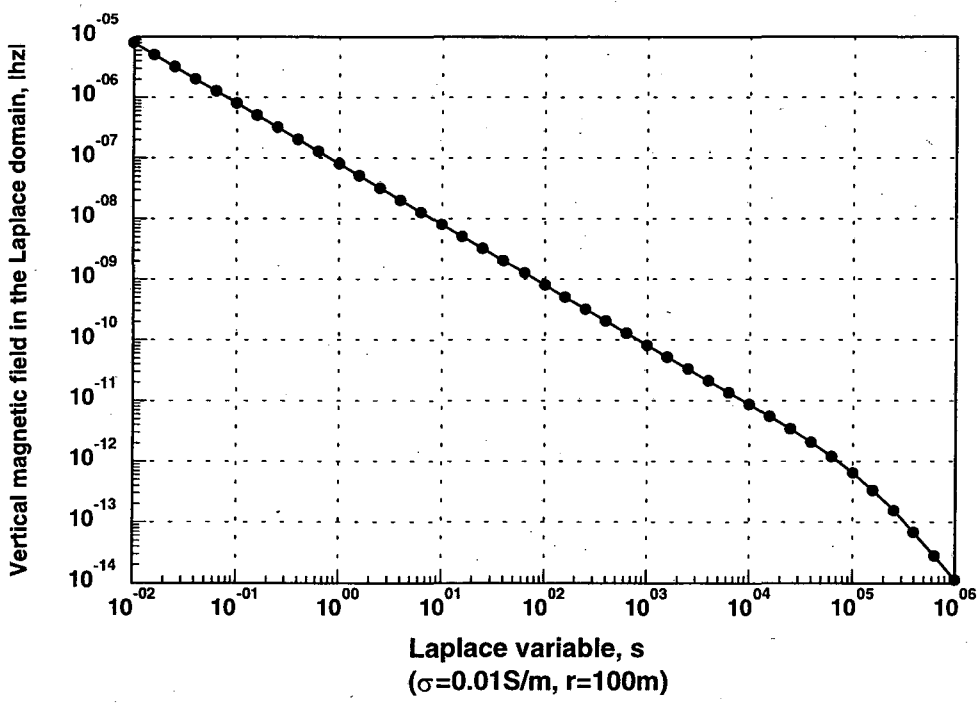

Fig.5 Vertical magnetic fields in the Laplace domain due to the VMD source (1A-m^2) on the homogeneous (0.01S/m) half space.

The coefficient matrix **A** becomes a large sparse matrix. In order to solve the set of linear equations, the incomplete Cholesky conjugate gradient (ICCG) method is used (Smith, 1996, for example). It is well known that the ICCG method is effective in solving a set of linear equations that has a large sparse matrix. In this work, FORTRAN subroutines for ICCG method developed by Dongarra et al. (1982) are used to solve the linear equations. The method used in the ICCG solver uses a preconditioner based on an incomplete LU factorization. These subroutines can be used to solve symmetric as well as non-symmetric systems.

After calculating the secondary electric fields, the secondary magnetic fields can be obtained using integral form of equation (43)

$$\oint \mathbf{e}^{(S)} \cdot dl = -\mu s \iint \mathbf{h}^{(S)} \cdot \mathbf{n} da \tag{63}$$

Each component of magnetic fields can be calculated by the approximated equations

$$h_x^{(S)}(i,j,k) = \frac{1}{\mu s}\left\{\frac{e_y^{(S)}(i,j,k+1) - e_y^{(S)}(i,j,k)}{\Delta z(k)} + \frac{e_z^{(S)}(i,j,k) - e_z^{(S)}(i,j+1,k)}{\Delta y(j)}\right\} \tag{64}$$

$$h_y^{(S)}(i,j,k) = \frac{1}{\mu s}\left\{\frac{e_x^{(S)}(i,j,k) - e_x^{(S)}(i,j,k+1)}{\Delta z(k)} + \frac{e_z^{(S)}(i+1,j,k) - e_z^{(S)}(i,j,k)}{\Delta x(i)}\right\} \tag{65}$$

$$h_z^{(S)}(i,j,k) = \frac{1}{\mu s}\left\{\frac{e_x^{(S)}(i,j+1,k) - e_x^{(S)}(i,j,k)}{\Delta y(j)} + \frac{e_y^{(S)}(i,j,k) - e_y^{(S)}(i+1,j,k)}{\Delta x(i)}\right\} \tag{66}$$

Finally total electric and magnetic fields can be calculated by equations (39) and (40).

Numerical examples

In order to test the computer program we developed, a simple three-dimensional model illustrated in Fig.6 is used. An equally spaced grid model $(20 \times 20 \times 20)$ is used to calculate the electromagnetic fields. As each grid spacing has a length of 20m, the model space becomes $380m \times 380m \times 380m$ in volume. In electromagnetic modeling, we have to consider the air region above the ground surface. The upper $380m \times 380m \times 120m$ volume is used as the air region that has a conductivity of 0 S/m, and the lower $380m \times 380m \times 260m$ volume is used as the earth region (0.01S/m) that contains an anomalous body (1 S/m).

Fig.7 shows the relation between the number of iterations and ICCG residual. We can see that the ICCG residual decreases smoothly. With the convergence criterion of ICCG residual set to 10^{-10}, 300 iterations are required and CPU time is about 260 sec to complete the calculation using a PC (266MHz Pentium II, 128MB memory).

The distributions of the secondary electric fields of x and y directions on the ground surface are shown in Fig.8 and Fig.9. The total electric fields on the ground surface are shown in Fig.10 and Fig.11.

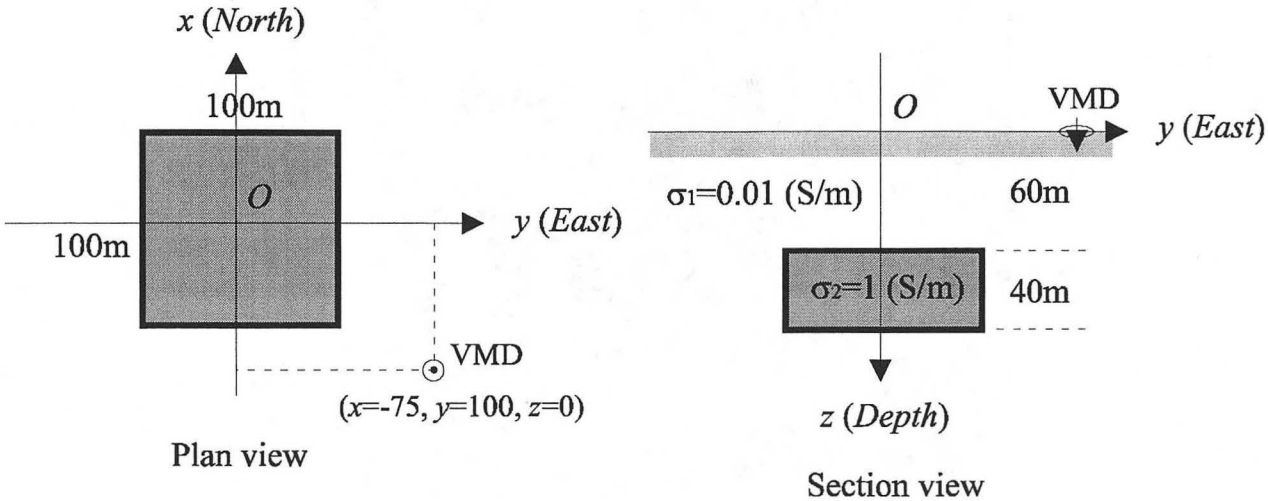

Fig.6 Three-dimensional conductivity body $(100m \times 100m \times 40m)$ in a homogeneous half space.

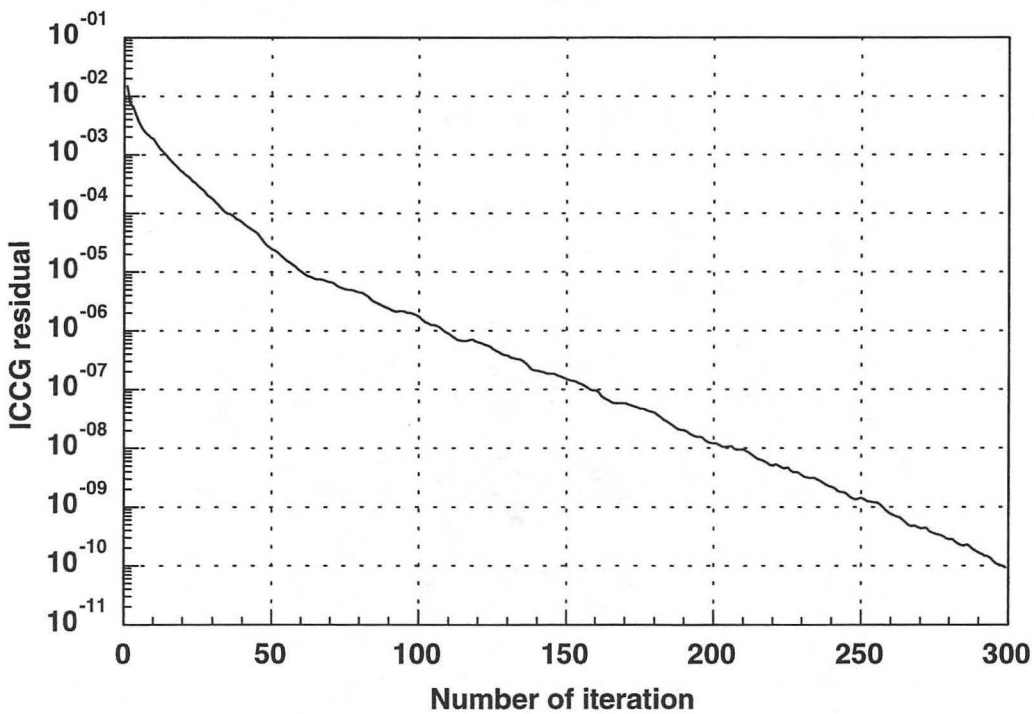

Fig.7 The relation between number of iteration and ICCG residual.

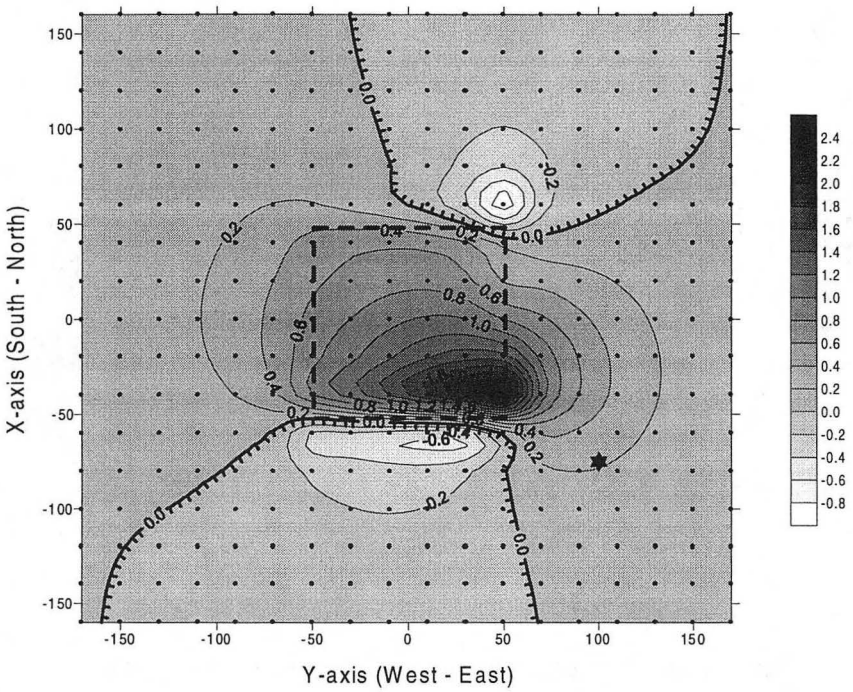

Fig.8 The secondary electric fields of x-direction on the ground surface, $e_x^{(S)} \times 10^{-12}$ $(s = 10^4)$.

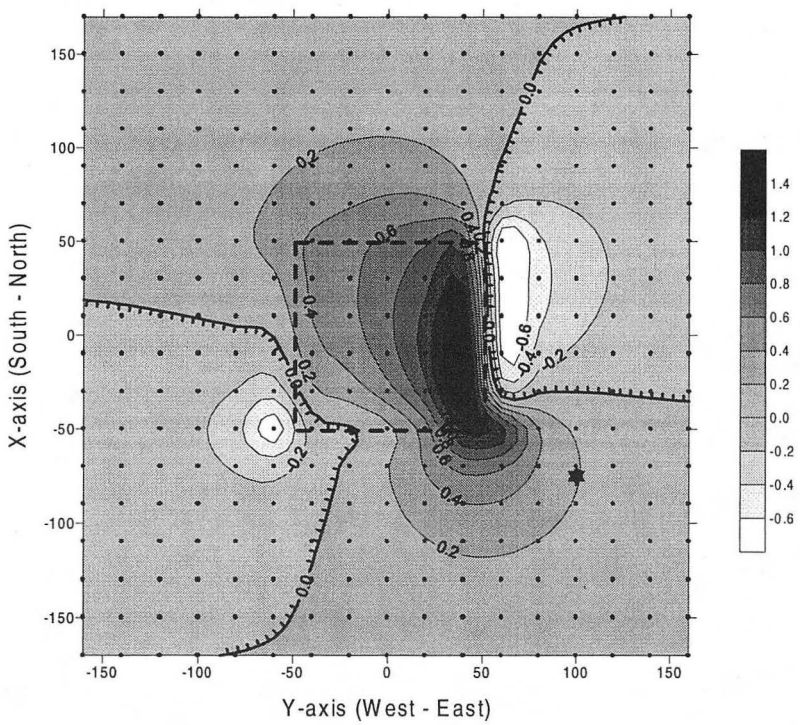

Fig.9 The secondary electric fields of y-direction on the ground surface, $e_y^{(S)} \times 10^{-12}$ $(s = 10^4)$.

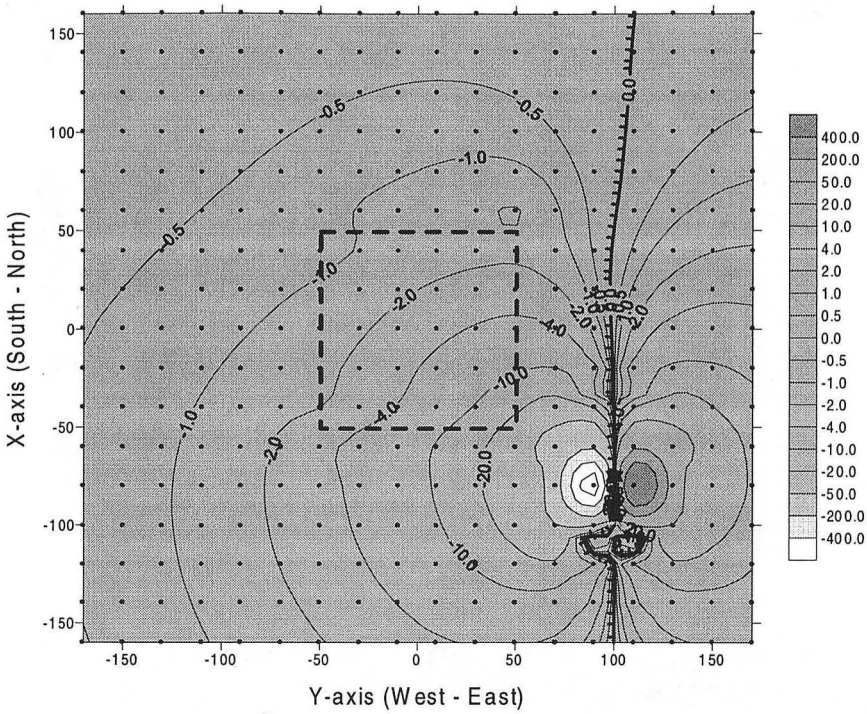

Fig.10 The total electric fields of x-direction on the ground surface, $e_x \times 10^{-12}$ $(s = 10^4)$.

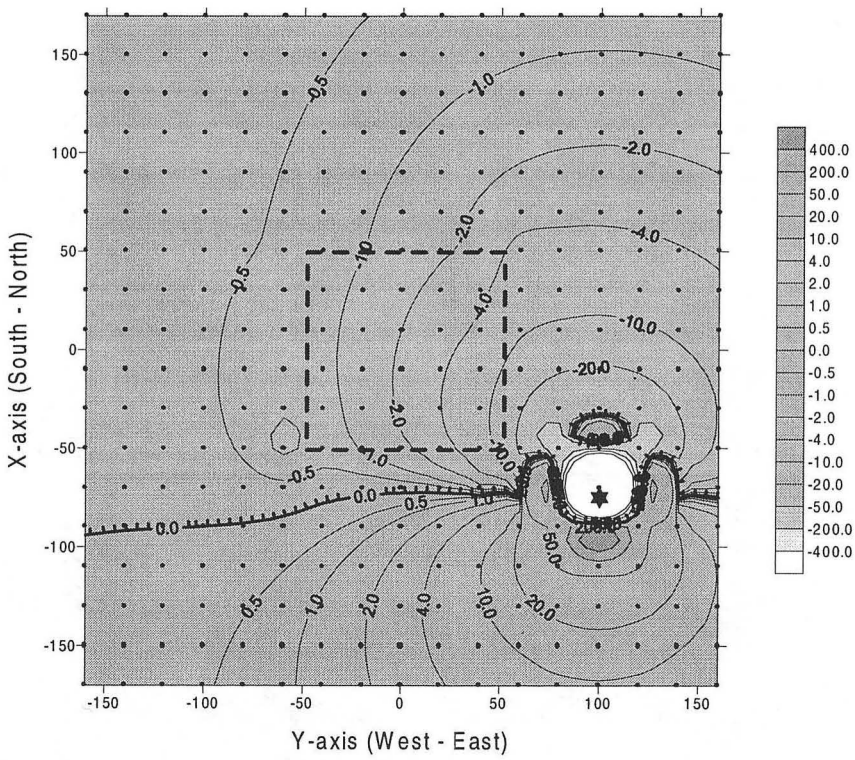

Fig.11 The total electric fields of y-direction on the ground surface, $e_y \times 10^{-12}$ $(s = 10^4)$.

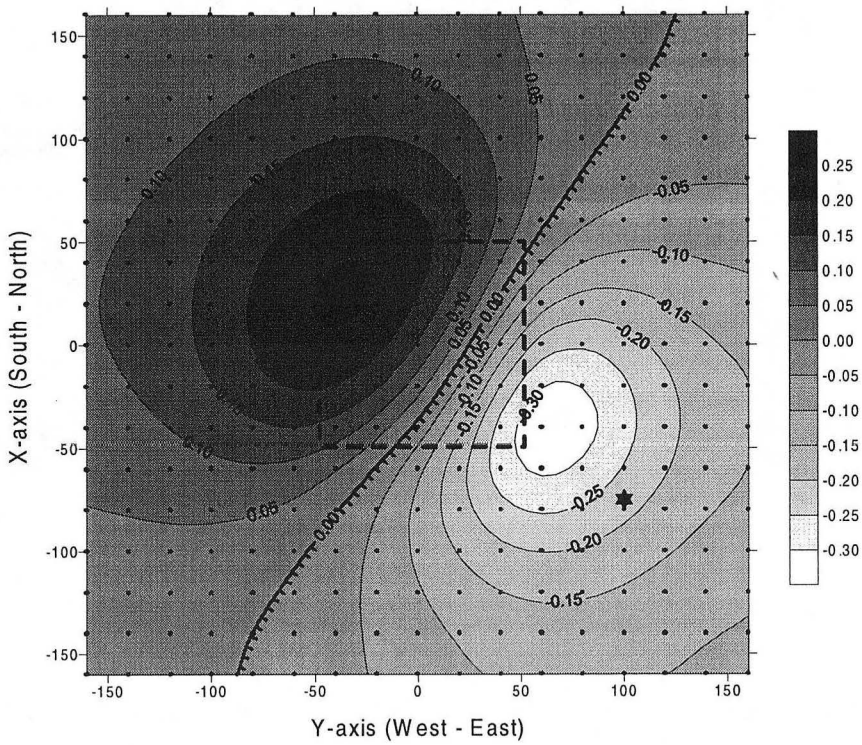

Fig.12 The second magnetic fields of z-direction on the ground surface, $h_z^{(S)} \times 10^{-12}$ $(s = 10^4)$.

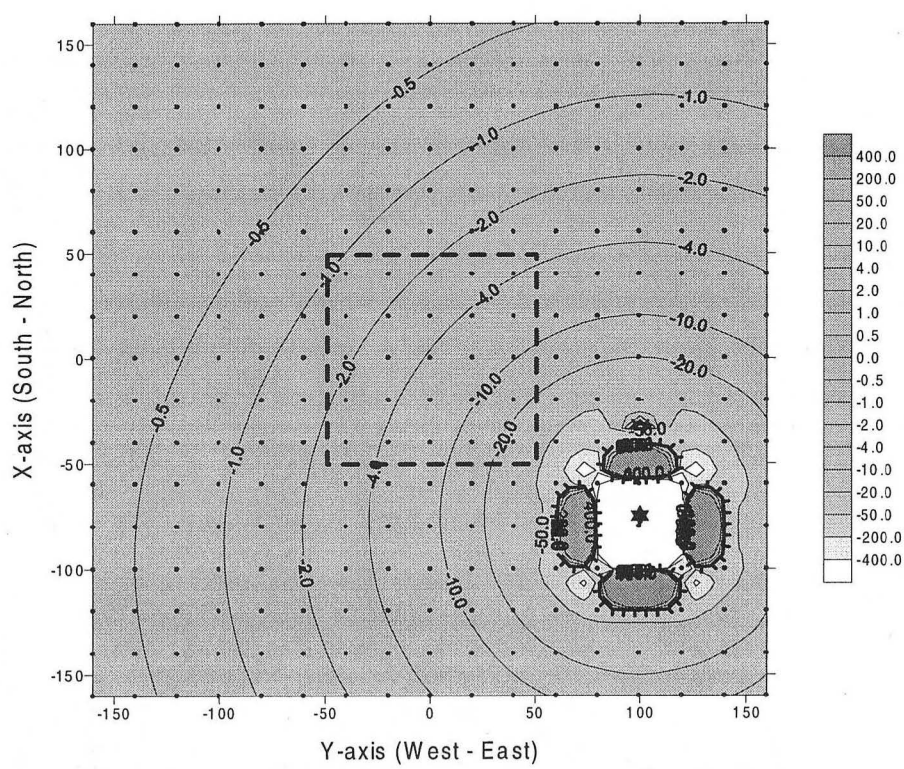

Fig.13 The total magnetic fields of z-direction on the ground surface, $h_z \times 10^{-12}$ $(s = 10^4)$.

In Figures 8 through Fig.11, the dashed-line-square indicates the location of anomalous conductive the body and black star indicates the location of the VMD source. From the distributions of the secondary electric field illustrated in Fig.8 and 9, we can see that a positive anomaly appears on the conductive body between two negative anomalies and maximum positive anomaly occurs at the nearest corner of anomalous conductive body.

In Figures 10 and 11, the total electric fields, both e_x and e_y, are almost divided into two (negative and positive) parts across the line y=100m and x=-75m respectively. There is no evident anomaly in the distributions of total electric fields because the magnitude of the secondary fields is very small compared to that of the primary field. However, we can see the distorted contour lines around the edges of anomalous conductive body.

Using equation (66) and the secondary electric fields on both the x and y directions (Figures 8 and 9), we can calculate the secondary magnetic field illustrated in Figure 12. In Figure 12, the maximum negative anomaly appears at the nearest corner of anomalous conductive body and the maximum positive anomaly appears at the opposite corner.

Figure 13 shows the total magnetic field in the z-direction on the ground surface due to anomalous conductive body. The distribution of the total magnetic fields becomes concentric circles with the center at the VMD source, because the secondary magnetic field is too small compared to the primary field.

Conclusion

We have developed a new technique to simulate electromagnetic fields of three-dimensional structures. The new technique is based on Maxwell's equations in the Laplace domain. The discretization of Maxwell's equations in the Laplace domain is performed by the finite difference method using a staggered grid. A numerical modeling code has been written based on the new approach to calculate electromagnetic fields due to 3-D anomalous body. The program can handle the permittivity distribution as well as the conductivity distribution and is applicable to 3-D transient electromagnetic inversion study in the future.

The new method requires less computer memory (almost half) than that used in other methods based on Maxwell's equations in the frequency domain. The computing speed is also faster than the frequency domain modeling using the same three-dimensional grid. This is because all components of electromagnetic fields in the Laplace domain are real numbers and all computation are performed in real arithmetic.

We believe that this technique will become an important tool for analyzing data obtained from transient electromagnetic survey in the future.

Acknowledgment

This study was supported in part by the Office of Basic Energy Sciences, Engineering and Geosciences Division of the U.S. Department of Energy under Contract No. DE-AC03-76SF00098. H. Mizunaga wishes to thank Prof. H. Frank Morrison for his offering an opportunity to conduct research at UC Berkeley and Lawrence Berkeley National Laboratory. This work was supported in part by Japan National Oil Corporation (JNOC).

References

Chen, Y. M., 1985, Generalized pulse-spectrum technique: *Geophysics*, **50**, 1664-1675.

Dongarra, J. J., Leaf, G. K. and Minkoff, M., 1982, A Fortran IV subroutine to solve large sparse general systems of linear equations: http://www.netlib.org/linalg/iccg-doc.

Guptasarma, D. and Singh, B., 1997, New digital linear filters for Hankel J_0 and J_1 transforms: *Geophysical Prospecting*, **45**, 745-762.

Nabighian, M. N., 1994, Electromagnetic Methods in applied Geophysics vol.1: *Society of Exploration Geophysicists*, 131-363.

Newman, G. A., and Alumbaugh, D.L., 1995, Frequency-domain modeling of airborne electromagnetic responses using staggered finite differences, *Geophys. Prosp.*, **43**, 1021-10412

Smith, J. T., 1996, Conservative modeling of 3-D electromagnetic fields, Part I: Properties and error analysis, *Geophysics*, **61**, 1308-1318.

Smith, J. T., 1996, Conservative modeling of 3-D electromagnetic fields, Part II: Biconjugate gradient solution and an accelerator, *Geophysics*, **61**,1319-1324.

Wang, T., and Hohmann, G. W., 1993, A finite-difference time-domain solution for three-dimensional electromagnetic modeling, *Geophysics*, **58**, 797-809.

Ernest Orlando Lawrence Berkeley National Laboratory
One Cyclotron Road | Berkeley, California 94720

Prepared for the U.S. Department of Energy under Contract No. DE-AC03-76SF00098